

Kenny Mahan

Mechanical Engineering Department,
Center for Life Cycle Engineering,
University of Maryland,
College Park, MD 20742

Yong Sun

Mechanical Engineering Department,
Center for Life Cycle Engineering,
University of Maryland,
College Park, MD 20742

Bongtae Han¹

Fellow ASME
Mechanical Engineering Department,
Center for Life Cycle Engineering,
University of Maryland,
College Park, MD 20742
e-mail: bthan@umd.edu

Sungwon Han

Mechanical Engineering Department,
Center for Life Cycle Engineering,
University of Maryland,
College Park, MD 20742

Mike Osterman

Mechanical Engineering Department,
Center for Life Cycle Engineering,
University of Maryland,
College Park, MD 20742

Adhesion and Puncture Strength of Polyurethane Coating Used to Mitigate Tin Whisker Growth

Reliability of conformal coatings used to mitigate tin whisker growth depends on their ability to contain tin whiskers. Two key material properties required to assess the reliability of a polyurethane coating are documented experimentally: adhesion strength and puncture strength. A modified blister test using a predefined blister area is employed to assess the adhesion strength and a puncture test is employed to evaluate the puncture strength of the coating. After measuring the properties at time zero, the coatings are subjected to accelerated testing conditions (high temperature/humidity storage and temperature cycling) and the degradations of the coating properties are documented.

[DOI: 10.1115/1.4026922]

Keywords: tin whisker, conformal coating, blister test, puncture test, adhesion strength, puncture strength, polyurethane coating, accelerated testing

1 Introduction

The ongoing movement to replace lead (Pb) from electronics has made pure tin plating a major choice for lead-free components. The issue with the pure tin plating is the single crystal metal hairlike growth from the tin surface, called the tin whisker [1,2]. Tin whiskers can be straight or kinked with diameters on the order of 1 to 5 μm [2]. They are electrically conductive and can bridge adjacent interconnect, causing circuit shortage, or they can be dislodged and obstruct or interconnect with other components. Tin whiskers are regarded as a major safety, reliability, and potential liability threat to high reliability electronics and associated hardware. The extensive review [3] of the tin whisker bibliography and mitigation practice provides good knowledge of tin whisker.

Several options are currently available to mitigate tin whisker growth [4]. One commonly implemented mitigation option is to apply a conformal coating over a tin coated area [5,6]. A conformal coating is a polymeric layer that can contain the whisker and prevent it from bridging adjacent interconnects. Even though conformal coatings cannot prevent tin whisker formation, it can reduce the rate of growth and contain the tin whisker with the electrically insulated coating [7]. The ability of different conformal coatings to suppress tin whisker formation and growth has been examined under long-term accelerated test conditions [8,9]. The study shows that whiskers can still penetrate the conformal coating at thin coated areas. Two key material properties required to assess the ability of a polyurethane coating to contain tin

whiskers are adhesion strength and puncture strength. The adhesion strength assesses the resistance to delamination between the coating and tin surface when a whisker begins to nucleate, while the puncture strength characterizes the coatings resistance to puncture of the whisker. Together the adhesion strength and puncture strength can be used to characterize the reliability of the coating.

In this paper, the adhesion strength and puncture strength of a conformal coating are determined experimentally. A polyurethane coating is selected for testing since it has been proven to mitigate tin whisker growth effectively [5,8,9]. A modified blister test using a predefined blister area larger than the pressure application hole is employed to assess the adhesion strength. A puncture test is employed to evaluate the puncture strength of the coating. The properties were determined after initial curing and then again after the samples are subjected to accelerated testing conditions (high temperature/humidity storage and temperature cycling) to investigate the effect of the conditions on the degradation of the coating.

2 Test Method

The two test methods, namely a modified blister test and a puncture test, are described briefly with their governing equations that relate experimentally measured quantities to adhesion strength and puncture strength.

2.1 Adhesion Strength Test: Modified Blister Test. Analytical solutions for the blister test configuration have been discussed in many different ways [10–14]. Let us consider a thin membrane adhered to a rigid substrate with a central hole for pressure application and a larger predefined area of low adhesion (Fig. 1). When pressure is applied, the thin membrane is assumed to take on a

¹Corresponding author.

Contributed by the Electronic and Photonic Packaging Division of ASME for publication in the JOURNAL OF ELECTRONIC PACKAGING. Manuscript received August 7, 2013; final manuscript received February 17, 2014; published online May 5, 2014. Assoc. Editor: Susan Lu.

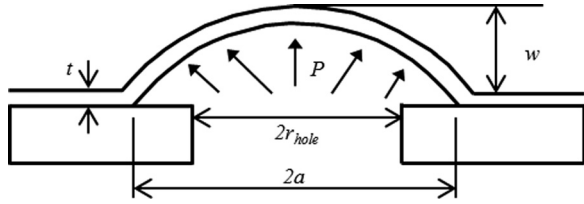


Fig. 1 Schematic illustration of a modified blister test specimen

spherical blister form when the deflection of the blister is much smaller than the opening radius. From the geometrical considerations in Fig. 1, the strain can be expressed as [15]

$$\varepsilon = \frac{2w^2}{3a^2} \quad (1)$$

where w is the blister height and a is the opening radius. Considering the force equilibrium, the normal stress of the thin membrane can be expressed as [15]

$$\sigma = \frac{Pa^2}{4wt} \quad (2)$$

where P is the applied pressure and t is the thickness of the membrane. As testing continues, the pressure is monotonically increased until a critical pressure, P_{crit} , is reached and the thin membrane delaminates from the surface. From the experimentally measured critical pressure, the adhesion strength is determined analytically.

The polyurethane conformal coating tested in this study has high adhesion strength, and usually deforms plastically during blister growth. If the conventional elastic blister model is used, the energy dissipated by plastic deformation will lead to an over-estimation of the adhesion strength. To cope with this behavior, the well-known work-hardening power law relationship is employed as the elastic-plastic constitutive equation.

The power law relationship can be expressed as

$$\varepsilon = \frac{\sigma_0}{E} \left(\frac{\sigma}{\sigma_0} \right)^{1/n} \quad \begin{array}{l} n = 1 \text{ for } \sigma < \sigma_0 \\ n = n_0 \text{ for } \sigma \geq \sigma_0 \end{array} \quad (3)$$

where σ_0 is the yield stress, n is the power-hardening exponent, and E is Young's modulus.

Substituting Eqs. (1) and (2) into (3), the blister height as a function of the pressure and opening radius can be expressed as

$$w = C_1^{-\frac{1}{2n+1}} P^{\frac{1}{2n+1}} a^{\frac{2n+2}{2n+1}} \quad \text{where } C_1 = \frac{2^{n+2} E^n t \sigma_0^{1-n}}{3^n} \quad \text{and} \quad \begin{array}{l} n = 1 \text{ for } \sigma < \sigma_0 \\ n = n_0 \text{ for } \sigma \geq \sigma_0 \end{array} \quad (4)$$

Using the notations shown in Fig. 1, the blister volume can be expressed as

$$V = C_2 \pi a^2 w \quad (5)$$

where C_2 is a numerical constant to accommodate the volume difference of the spherical cap due to the clamped end condition of the blister; $C_2 = 0.518$ for a typical Poisson's ratio of polymers has been reported in the literature [10,11,16].

The energy release rate, G , is a measure of the energy available for an increment of crack extension, and is an indication of the adhesion strength [17]. Following the procedures established in

Refs. [10,11,16,18], the energy release rate during delamination can be expressed by

$$G = \frac{3n+2}{n+1} \frac{PV}{2\pi a^2} \quad \text{where } \begin{array}{l} n = 1 \text{ for } \sigma < \sigma_0 \\ n = n_0 \text{ for } \sigma \geq \sigma_0 \end{array} \quad (6)$$

Using Eqs. (5) and (4), the energy release rate can be expressed in terms of the experimental parameters (pressure, opening radius, and material properties) as [18]

$$G = \frac{3n+2}{2n+2} C_1^{-\frac{1}{2n+1}} C_2 (Pa)^{\frac{2n+2}{2n+1}} \quad \begin{array}{l} n = 1 \text{ for } \sigma < \sigma_0 \\ n = n_0 \text{ for } \sigma \geq \sigma_0 \end{array} \quad (7)$$

2.2 Puncture Strength Test. In general, the puncture strength of a coating depends on the force required for a tin whisker to puncture the coating, and the contact area between the two surfaces. The puncture strength of polymer films can be determined experimentally by measuring the force required for a probe to puncture the coating normalized by the probe perimeter [19]

$$T_p = F_p / P_p \quad (8)$$

where T_p is the puncture strength, F_p is the puncture force, and P_p is the probe perimeter. When testing with a flat probe tip [19]

$$T_p = F_p / 2\pi r \quad (9)$$

where r is the probe radius. The above definition results in units of N/m. When testing with flat probe tips, the puncture strength is linearly proportional to the probe diameter [19].

3 Experimental Procedure

3.1 Modified Blister Test. From Eq. (7), it is obvious that the opening radius is critical to accurate determination of the adhesion strength. In conventional blister testing, the hole in the substrate used for pressure application is defined as the opening radius (r_{hole} in Fig. 1). After curing the conformal coating on the substrate, any excess adhesive between the walls of the pressure hole will directly affect the adhesive strength of the specimen. To address this issue, an opening radius larger than the pressure application hole is created with a low adhesion release agent before the test (a in Fig. 1). A procedure developed to produce an accurate opening radius while accommodating the highly "acidic" environment of tin electroplating is presented below.

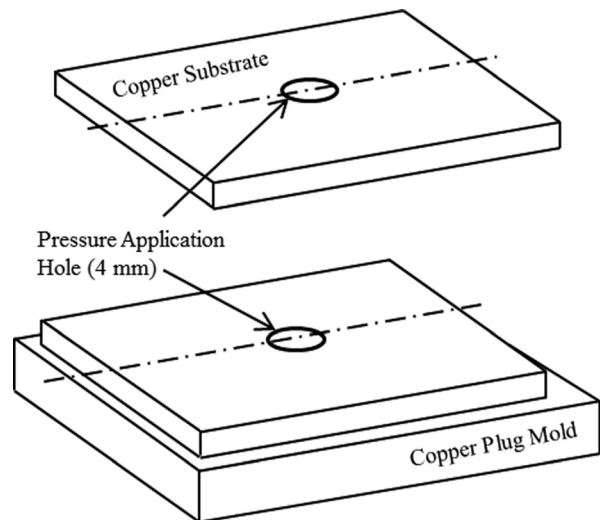


Fig. 2 3D view of (a) copper substrate and (b) copper plug mold

Figure 2 shows a simplified schematic view of the rigid copper substrate with a 4 mm diameter pressure application hole which will act as a base for tin plating, and the rigid copper plug mold used to form the epoxy plugs. Before the tin plating process can begin, the four pressure application holes in the rigid copper substrate must be temporarily filled with an epoxy material as seen in Fig. 3. The purpose of creating a temporary epoxy plug is twofold: (1) prevent tin from being plated on the inner perimeter of the pressure hole and (2) create a level surface for applying the release agent and conformal coating layers. The plug mold defines the shape of the temporary epoxy plug, allowing for easy epoxy injection and removal of the plug after curing the conformal coating layer.

To facilitate easy separation of the plug, a release agent (20-8185-002 Release Agent: Buehler) is applied on the surfaces of the holes. Next the substrate is placed with the side to be tin-plated face down and the plug mold aligned on top of the substrate. A two-part epoxy (EpoKwick Resin/Hardener: Buehler) is mixed in a 5:1 ratio and injected into the hole and allowed to cure at room temperature for 24 h. After curing, the surface is grinded and polished to remove excess epoxy and to prepare the surface for tin plating.

A tin plating bath solution is employed with tin attached to the anode end of a power supply and the sample to be plated attached to the cathode side. When voltage is applied, the metal is oxidized at the anode to form metal ions, and transferred through electrolyte to a negatively charged cathode to be reduced on its surface. After the process the copper substrate has a thin layer of tin on its surface as illustrated in Fig. 4(a). Figure 4 depicts the cross-sectional view of the sample preparation process for one test hole in Fig. 2.

The release agent and coating application process is also depicted in Fig. 4. After the plating process is completed, a circular mask is placed concentrically around the pressure application hole (Fig. 4(b)). Next a small layer of release agent is placed inside the mask and allowed to dry. The addition of the release agent layer significantly reduces the adhesive strength around the pressure application hole. Before testing, a small preload pressure is first applied to debond the release agent area at a very low pressure. This creates a well-defined, accurate opening radius at the perimeter of the release agent area.

Upon removal of the mask, a shim is placed around the top of the substrate, and a thin layer of the conformal coating is applied and allowed to cure at room temperature for 24 h (Fig. 4(c)). Finally, the plug mold is removed to clear the pressure port for testing leaving the final blister test specimen (Fig. 4(d)).

3.1.1 Experimental Setup and Test Procedure. A schematic diagram and actual test setup employed for the adhesion strength test are seen in Figs. 5 and 6, respectively. A conformal coating thickness of $50\ \mu\text{m}$ and a crack opening radius of $a = 3.2\ \text{mm}$ are used for the test. The blister test specimen is aligned over a pressure port. A pressure regulator (ER3000: Tescom) applies

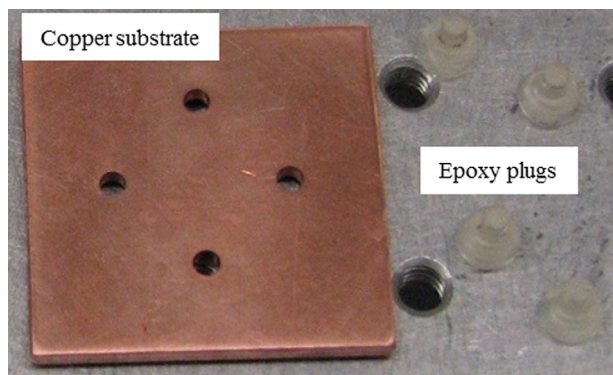


Fig. 3 Copper substrate with epoxy plugs

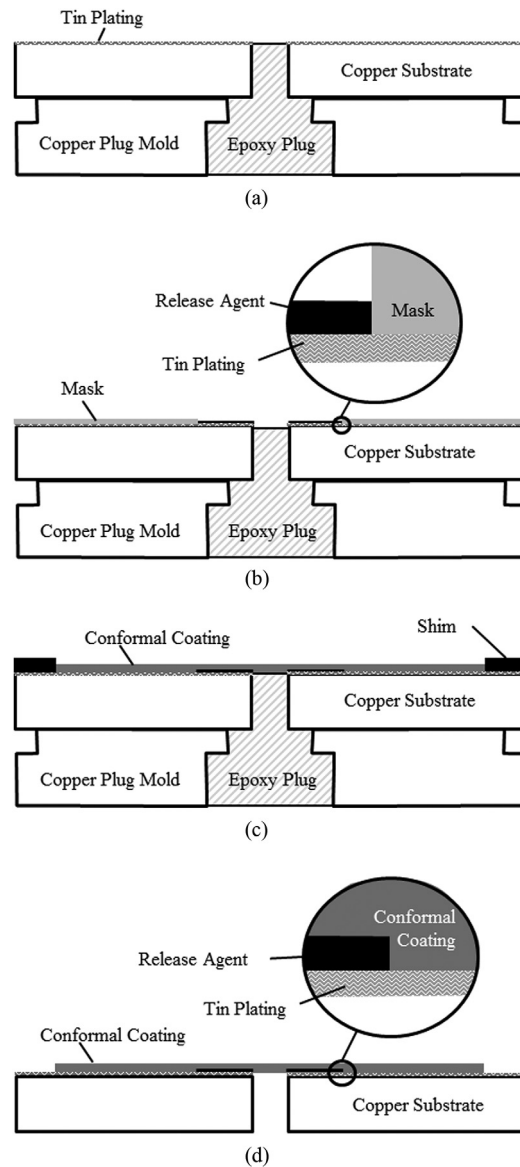


Fig. 4 Schematic cross sectional view of sample preparation process: (a) tin plated substrate and plug mold, (b) temporary mask and release agent application, (c) temporary shim for conformal coating curing, and (d) final blister test specimen

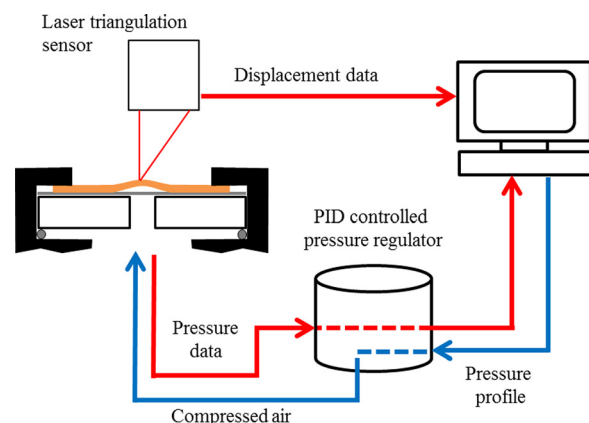


Fig. 5 Schematic diagram of the blister test setup

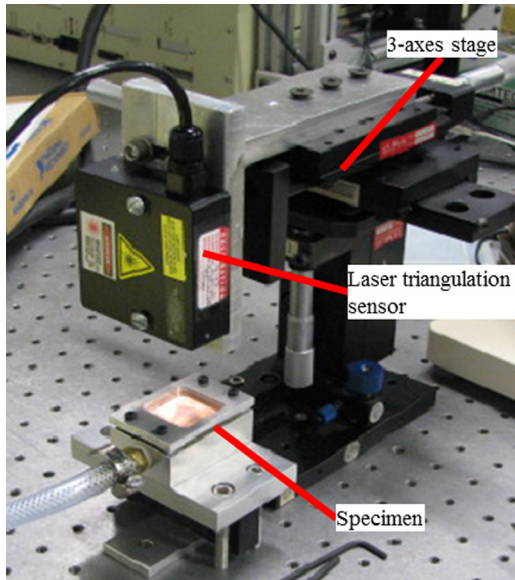


Fig. 6 Blister test setup

pressure at 0.1 psi/s and records the pressure to an accuracy of 0.1 psi. A laser triangulation sensor (LTC-050-10-SA: MTI instrument) simultaneously records the blister height within $2\ \mu\text{m}$. As the pressure increases monotonically, the blister continues to grow until a critical pressure is reached and the film delaminates from the tin-plated surface. The critical height and pressure can be determined from the pressure versus blister height results.

3.2 Puncture Test. For puncture testing, a thin film conformal coating specimen is required. A nonstick, Teflon substrate was placed on a level surface, and a shim of a desired film height placed on top. Next a spray conformal coating was transferred to a test tube, and then poured slowly onto the Teflon substrate. Any excess coating above the shim was removed to create a level film thickness. Extra care was also given to removing any excess bubbles that formed on top of the coating. The coating was then allowed to cure, diced into test specimens, and removed from the Teflon substrate.

3.2.1 Experimental Setup and Test Procedure. A schematic diagram and actual test setup employed for the puncture test setup is depicted in Figs. 7 and 8, respectively. The test probe is fitted to a 10N load cell on the cross head of an Instron test stand. The load cell is accurate to $\pm 0.05\ \text{N}$. A conformal coating of $50\ \mu\text{m}$ thickness is clamped between two aluminum plates with central test holes. The radius of this hole does not affect the puncture strength. An x - y stage aligns the probe in the center of the test hole before testing.

After alignment, the probe is extended at a rate of $0.5\ \text{mm/min}$ into the coating. The probe extends into the coating until a critical

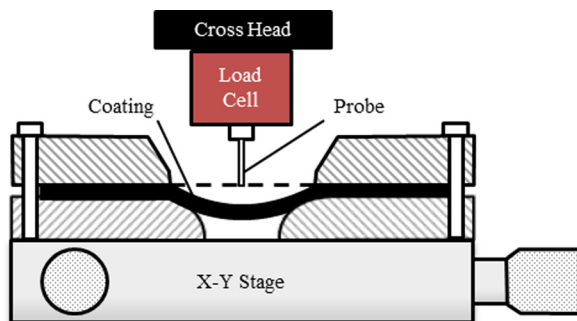


Fig. 7 Schematic diagram of the puncture test setup

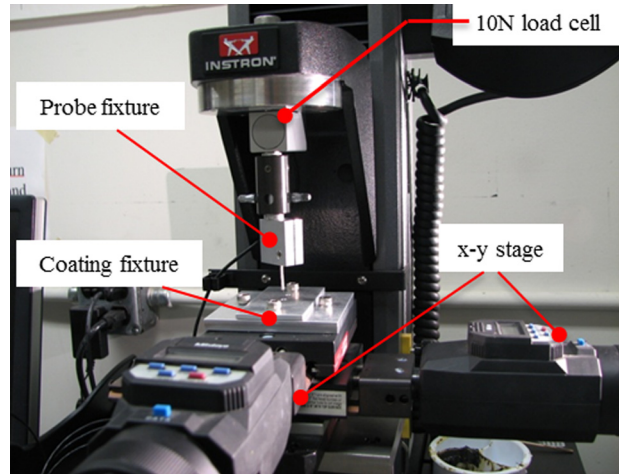


Fig. 8 Puncture test setup

puncture force is reached and the probe punctures the coating. The load and displacement data are measured simultaneously.

Test probes with three different radii are used for testing: $50\ \mu\text{m}$, $65\ \mu\text{m}$, and $80\ \mu\text{m}$. Probes with flat tips are employed to ensure repeatability of the experimental results.

4 Experimental Results

The two properties of the polyurethane conformal coating are characterized at room temperature first, and then after subjecting the coatings to two accelerated testing environments: high temperature and humidity (T/H) storage and temperature cycling (T/C).

4.1 Adhesion Strength. Two representative blister height versus pressure tests for the polyurethane coating prior to aging are shown in Fig. 9. The critical pressure is determined from the discontinuity of the blister height versus pressure graph. The critical pressure for the sample shown in Fig. 9 is 25 and 27 psi, respectively.

An advantage of the blister testing formation is that the initial portion of the elastoplastic properties of the coating. The unknown elastoplastic properties are the modulus, E , the hardening constant, n , and the yield strength, σ_y . To determine the elastoplastic

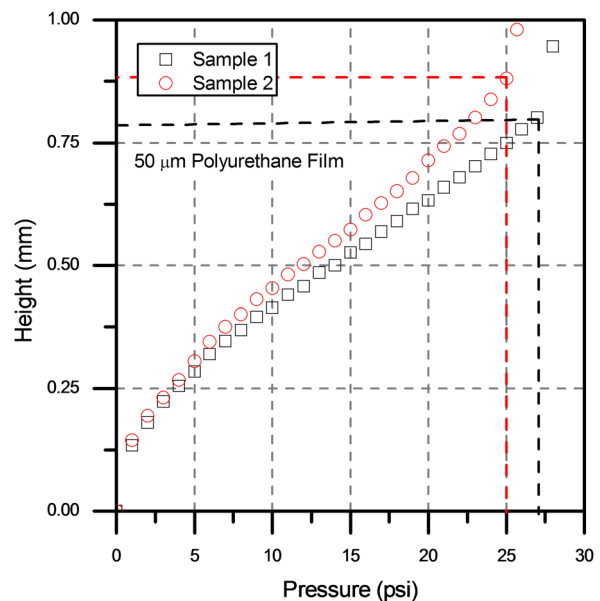


Fig. 9 Typical pressure versus blister height results for the blister test of a polyurethane conformal coating before aging

properties of the coating, a nonlinear regression analysis is performed to fit the experimental data to the analytical height from Eq. (4). Before the nonlinear regression analysis, the blister height versus pressure results was smoothed using the well-known Savitzky–Golay method.

A two part process is then employed to extract the elastoplastic properties. The modulus is determined first by using a nonlinear regression to fit the initial, elastic portion of the pressure versus blister height curve. Setting $n=1$ in Eq. (4) reduces the blister height analytical equation to the linear elastic relationship which is valid before the stress is greater than the yield stress.

Using the modulus from the elastic fit, a second nonlinear regression is performed over the entire elastoplastic curve to determine the hardening constant and the yield strength of the coating. The results of the fit are shown in Fig. 10. The resulting elastoplastic properties are listed below:

$$E = 956 \text{ MPa}$$

$$n = 0.333$$

$$\sigma_y = 5.90 \text{ MPa}$$

With the elastoplastic material properties, and the critical pressure from the experiment, the adhesion strength of the polyurethane/tin plating interface before aging is calculated by Eq. (7)

$$G = 94.9 \pm 11 \text{ J/m}^2$$

4.1.1 Accelerated Testing Results. The blister test samples were subjected to a suggested JEDEC T/H standard for tin whiskers [20] of 55 °C/85% RH and tested after 0, 1000, and 2000 h. Figure 11 shows how the average adhesion strength changes with time in T/H testing conditions. After 1000 h of T/H conditions, the adhesion strength increased by 40%. It is speculated that the initial increase in adhesion strength is caused by additional crosslinking of the polymer coating. After another 1000 h in the chamber, the coating did not degrade and the adhesion strength remains nearly constant.

Another set of blister test samples were subjected a temperature cycling condition. The suggested JEDEC T/C standard for tin whiskers is -55 °C to 85 °C. Due to the slow rate of degradation, a harsher test condition, -55 °C to 125 °C, was employed. Samples were then tested after 0, 500, and 1000 cycles in the T/C testing chamber. Figure 12 shows how the average adhesion strength changes with T/C testing cycles. After 500 cycles, the adhesion

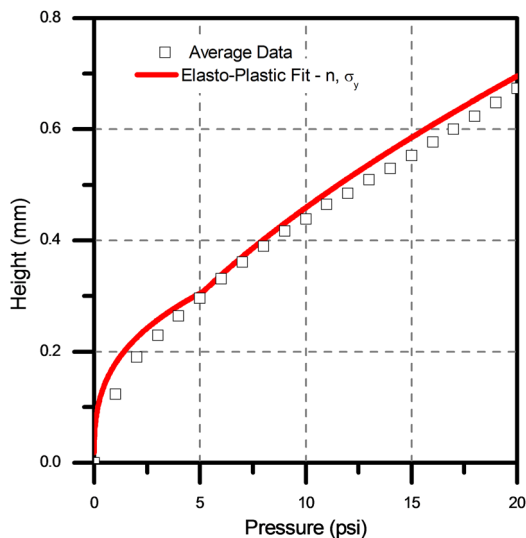


Fig. 10 Nonlinear regression results of the elastoplastic curve to determine the hardening constant and yield strength of the coating

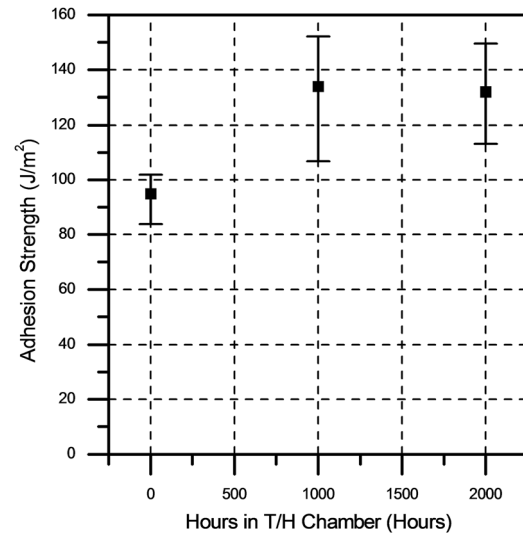


Fig. 11 Adhesion strength versus hours in a T/H chamber

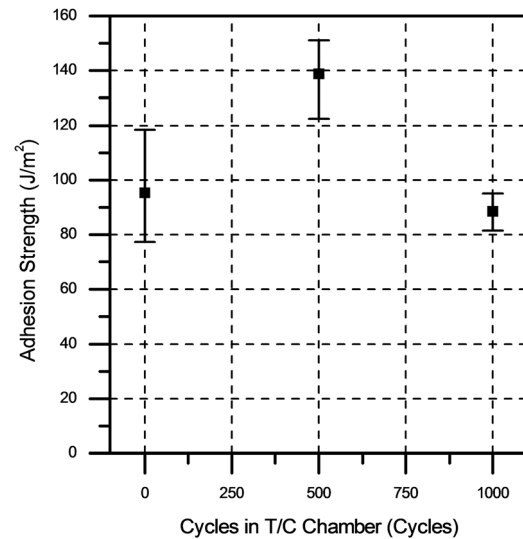


Fig. 12 Adhesion strength versus cycles in a T/C chamber

strength increased 27%. Again, this may be attributed to additional crosslinking of the polymer coating. Over the next 500 cycles the adhesion strength degrades by 22%.

4.2 Puncture Strength. Typical puncture force versus deflection results for the polyurethane coating are shown in Fig. 13 for three different probe radii and the corresponding puncture strength results are recorded in Table 1. As seen in the table, the puncture strength of the coating has a variation of less than 3% with probe radii. It follows that for a given whisker radius, the puncture force of the coating can be calculated from the puncture strength using Eq. (9).

Puncture test samples were subjected to IPC standard [21] T/H testing condition of 85 °C/95% RH, and tested after 0, 168 h, 336 h, and 504 h in the testing chamber. Figure 14 shows that the average puncture strength of the coating steadily decreased with time in this accelerated environment.

5 Discussions: Failure Modes

This paper has focused on the failure mechanisms due to tin whisker nucleation and growth from underneath the coating as seen in Fig. 15. As discussed, the puncture strength characterizes

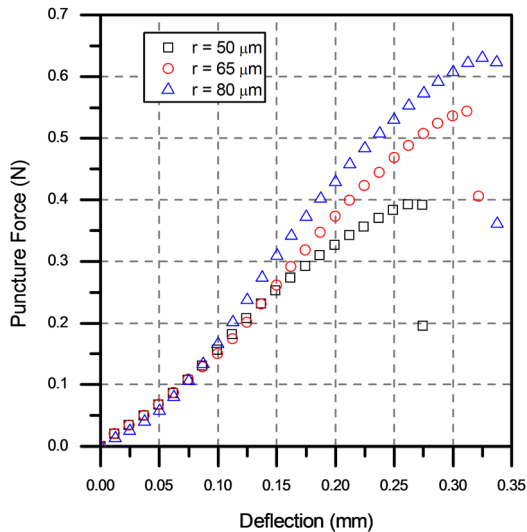


Fig. 13 Typical load versus deflection results for the puncture test of a polyurethane conformal coating

Table 1 Puncture strength with different probe radii

Probe radius (μm)	Puncture strength (J/m^2)
50	1343 ± 78
65	1341 ± 24
80	1282 ± 19

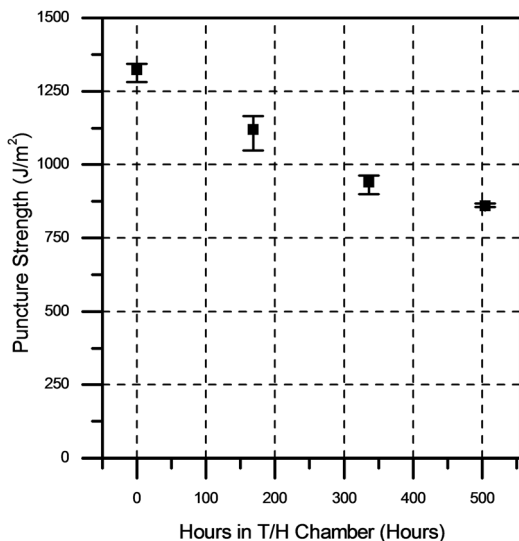


Fig. 14 Puncture strength versus hours in a T/H chamber

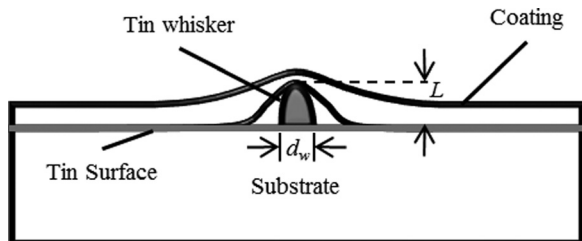


Fig. 15 Schematic of tin whisker nucleating on tin coated substrate

the failure of the conformal coating due to cohesive penetration by tin whisker nucleation. The puncture force of the coating can be calculated when the puncture strength, T_p , and the whisker radius, d_w , are known by the following equation [19]:

$$F_p = \pi d_w T_p \quad (10)$$

As the whisker continues to grow from underneath the coating, a competing mechanism to puncture, buckling, is introduced. If the whisker buckles before reaching the puncture strength of the coating, the whisker will be contained within the coating, preventing a failure due to penetration. To compare the competing mechanisms, the buckling force of a tin whisker can be calculated by [6]

$$F_b = \frac{\pi^3 E_w d_w^4}{32 L^2} \quad (11)$$

where L is the length of the whisker, E_w is the modulus of the tin whisker, and d_w is the diameter of the whisker. From Eqs. (10) and (11), we can see the puncture force is independent of the whisker length and the buckling force is inversely proportional to the whisker length squared.

Figure 16 depicts the puncture and buckling force plotted versus the whisker length. In the figure, three different whisker diameters are considered, $d_w = 2, 4, 6 \mu\text{m}$, the tin whisker modulus is assumed to be $E_w = 42 \text{ GPa}$ [3], and the puncture strength of the tested conformal coating is $T_p = 1322 \text{ J}/\text{m}^2$. For a given whisker diameter and puncture strength, there exists a critical whisker length at which the critical force required to puncture the coating becomes larger than the critical buckling force

$$L_{\text{Critical}} = \sqrt{\frac{\pi^2 E_w d_w^3}{32 T_p}} \quad (12)$$

Figure 17 plots the critical whisker length for buckling versus whisker diameter. For whiskers longer than the critical whisker length, the whiskers buckle and are contained by the conformal coating and do not result in failure. The critical whisker length increases with increasing whisker diameter therefore as expected, thinner diameter whiskers are much easier to contain. So given the above coating properties, a $6 \mu\text{m}$ diameter whisker will buckle and be contained if it grows longer than $150 \mu\text{m}$ in length. This

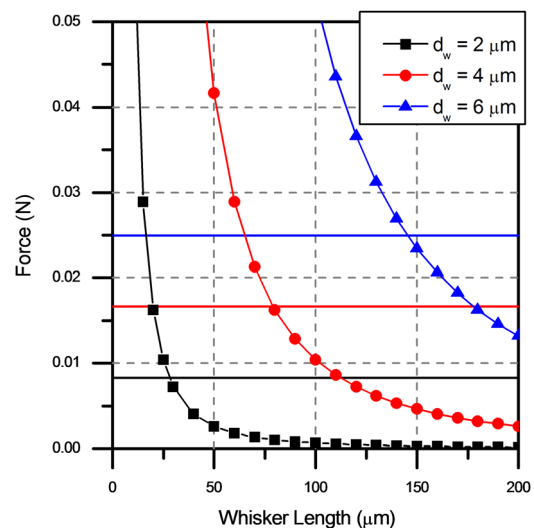


Fig. 16 Puncture force and buckling force versus whisker length

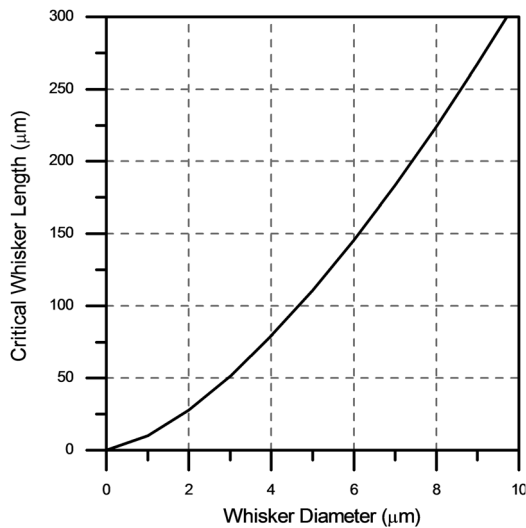


Fig. 17 Critical whisker length for buckling versus whisker diameter

approach could be applied to set a design point to identify required thicknesses of conformal coatings.

The adhesion strength between the coating and tin layer also affects the reliability of the coating because whiskers can escape from exfoliated areas of the coating. Additionally, delaminated openings resulting from a growing whisker lifting the coating affect the delamination configuration and alter the puncture force of the whisker. As the delaminated area increases, both the puncture and buckling forces are reduced. Because of the delaminated surface, the critical whisker length would increase significantly compared to the puncture strength, allowing for even longer whiskers to be contained.

Future work can expand on this concept through advanced numerical modeling to determine what will occur once a tin whisker nucleates on a conformally coated surface. A sequential approach can be applied considering a contact analysis and an indentation analysis for the initial nucleation of the whisker into the coating. This initial stress analysis determines the stress/strain distribution around the whisker tip as well as the total force exerted on the whisker. The former can be compared to the puncture strength of the coating to assess if puncture occurs first, while the latter can be input to a buckling analysis. The lifting force on the whisker can also be used to calculate the stress along the interface of the coating/tin plating surface. If the stresses at the interface are large enough to overcome the adhesion strength of the interface, delamination occurs, which redefines the deformation configuration of the analysis.

6 Conclusion

Two key material properties required to assess the reliability of a polyurethane coating were obtained: adhesion strength by blister testing and puncture strength by puncture test. A procedure to prepare blister samples for tin-plated surfaces was proposed, including a method for creating a well-defined predefined area. A blister test procedure was employed to determine the elasto-plastic properties of a urethane conformal coating. The elasto-plastic properties of conformal coatings were then considered in adhesion strength calculations leading to a more realistic determination of the adhesion strength. A puncture test was employed to determine the puncture strength of the coating. Blister test and puncture test samples were tested before and after accelerated testing conditions and the degradation of the coating properties was reported.

Adhesion strength samples in both T/H and T/C environments both experienced an initial increase in the adhesion strength ranging from 27% to 40%. This increase in adhesion strength is speculated to be attributed to additional cross-linking of the polymer coating. Continued T/H testing resulted in little change in the adhesion strength, whereas the T/C testing environment resulted in 22% decrease in adhesion strength over the next 500 cycles. The puncture strength saw 35% decrease in strength after 500 h in a T/H testing environment. The results indicated that a polyurethane coating would be an effective solution to mitigate the tin whisker growth problem.

Acknowledgment

This work was supported by the Center for Advanced Life Cycle Engineering (CALCE) of the University of Maryland. Their support is acknowledged gratefully.

References

- [1] Compton, K., Mendizza, A., and Arnold, S., 1951, "Filamentary Growths on Metal Surfaces—Whiskers," *Corrosion*, 7(10), pp. 327–334.
- [2] Schroeder, V., Bush, P., Williams, M., Vo, N., and Reynolds, H. L., 2006, "Tin Whisker Test Method Development," *IEEE Trans. Electron. Packag. Manuf.*, 29(4), pp. 231–238.
- [3] Galyon, G. T., 2005, "Annotated Tin Whisker Bibliography and Anthology," *IEEE Trans. Electron. Packag. Manuf.*, 28(1), pp. 94–122.
- [4] Osterman, M., 2002, "Mitigation Strategies for Tin Whiskers," CALCE EPSC, College Park, MD, <http://www.calce.umd.edu/lead-free/tin-whiskers/TIN-WHISKERMITIGATION.pdf>
- [5] Fox, W., and Woody, L., 2010, "Conformal Coatings for Tin Whisker Risk Management," IPC APEX EXPO Technical Conference, Las Vegas, NV, April 6–9, pp. 890–920.
- [6] Kadesch, J. S., and Leidecker, H., 2000, "Effects of Conformal Coat on Tin Whisker Growth," 37th IMAPS Nordic Annual Conference, Helsingor, Finland, September 10–13, Paper No. S31-01, pp. 108–116.
- [7] Kadesch, J. S., and Brusse, J., 2001, "The Continuing Dangers of Tin Whiskers and Attempts to Control Them With Conformal Coating," NASA EEE Links Newsletter, July.
- [8] Woodrow, T. A., and Ledbury, E. A., 2005, "Evaluation of Conformal Coatings as a Tin Whisker Mitigation Strategy," IPC/JEDEC 8th International Conference on Lead-Free Electronic Components and Assemblies, San Jose, CA, April 18–20.
- [9] Woodrow, T. A., and Ledbury, E. A., 2006, "Evaluation of Conformal Coatings as a Tin Whisker Mitigation Strategy, Part 2," SMTA International Conference, Rosemont, IL, September 24–28.
- [10] Gent, A. N., and Lewandowski, L. H., 1987, "Blow-Off Pressures for Adhering Layers," *J. Appl. Polym. Sci.*, 33(5), pp. 1567–1577.
- [11] Shirani, A., and Liechti, K., 1998, "A Calibrated Fracture Process Zone Model for Thin Film Blistering," *Int. J. Fract.*, 93(1), pp. 281–314.
- [12] Dannenberg, H., 1961, "Measurement of Adhesion by a Blister Method," *J. Appl. Polym. Sci.*, 5(14), pp. 125–134.
- [13] Williams, M., 1969, "The Continuum Interpretation for Fracture and Adhesion," *J. Appl. Polym. Sci.*, 13(1), pp. 29–40.
- [14] Fernando, M., and Kinloch, A., 1990, "Use of the 'Inverted-Blister' Test to Study the Adhesion of Photopolymers," *Int. J. Adhes. Adhes.*, 10(2), pp. 69–76.
- [15] Hinkley, J. A., 1983, "A Blister Test for Adhesion of Polymer Films to SiO₂," *J. Adhes.*, 16(2), pp. 115–126.
- [16] Hencky, H., 1915, "Über den Spannungszustand in Kreisrunden Platten mit Verschwindende Biegesteifigkeit," *Z. Angew. Math. Phys.*, 63, pp. 311–317.
- [17] Anderson, T. L., 2005, *Fracture Mechanics: Fundamentals and Applications*, Taylor & Francis Group, Boca Raton, FL.
- [18] Mahan, K., Sun, Y., Han, B., Han, S., and Osterman, M., 2011, "PoF Model of Conformal Coating Against Tin Whisker Growth: Performance Evaluation Under Operating and Storage Conditions," Center for Advanced Life Cycle Engineering (CALCE), College Park, MD, Paper No. C11-06.
- [19] Nguyen, C., and Vu-Khanh, T., 2004, "Mechanics and Mechanisms of Puncture of Elastomer Membranes," *J. Mater. Sci.*, 39(24), pp. 7361–7364.
- [20] JESD201, 2006, "Environmental Acceptance Requirements for Tin Whisker Susceptibility of Tin and Tin Alloy Surface Finishes," JEDEC Solid State Technology Association, Arlington, VA, JEDEC Standard No. 201.
- [21] IPC Cleaning and Coating Committee, 2008, "Qualification and Performance of Electrical Insulating Compound for Printed Wiring Assemblies," IPC Association Connecting Electronics Industries, Bannockburn, IL, Report No. IPC-CC-830B.